TMA4220: Numerical solution of partial differential equations by element methods

Steady Convection-Diffusion Equation: A One-Dimensional Example

March 14, 2002

Einar M. Rønquist
Department of Mathematical Sciences
NTNU, N-7491 Trondheim, Norway

1 A steady convection-diffusion problem

Let us consider the one-dimensional convection-diffusion problem

$$\begin{aligned} -\kappa\, u_{xx} + U\, u_x &= f \quad in\ \ \Omega = (0,1)\ , && (1)\\ u(0) &= 0\ , && (2)\\ u(1) &= 1\ . && (3) \end{aligned}$$

Here, u represents temperature, κ represents the thermal conductivity, f represents a volumetric heat source, and U is a constant. We can think of U as representing a divergence-free (or incompressible) velocity field which is given. Dirichlet boundary conditions are prescribed at $x = 0$ and $x = 1$. The length of the domain is $L = 1$.

The (dimensionless) Peclet number associated with the physical problem is

$$P = \frac{U\, L}{\kappa}\ , \tag{4}$$

and it measures the importance of convection relative to diffusion.

1.1 The case with $f = 0$ and $U = 1$

Let us first consider the case with $f = 0$. The analytical solution for this case is given as

$$u(x) = \frac{e^{x/\varepsilon} - 1}{e^{1/\varepsilon} - 1} \tag{5}$$

where

$$\varepsilon = \frac{\kappa}{U}\ . \tag{6}$$

Let us further assume that $U = 1$, i.e., the "wind" is blowing from left to right. If ε is small compared to L, the length of our domain, we get a boundary layer of thickness ε near $x = 1$. Outside this thin boundary layer, the solution is approximately equal to zero.

A useful way of representing this type of solution is by considering the total solution as the sum of two parts: an *inner* boundary layer solution, u_{inner} , given by (5), and an *outer* solution $u_{outer} = 0$, i.e.,

$$u(x) = u_{inner} + u_{outer}\ . \tag{7}$$

Note that, outside the boundary layer, the diffusion term $\kappa\, u_{xx}$ is small compared to the convection term $U\, u_x$. Hence, outside the boundary layer, $u_x \sim f/U = 0$. Together with the boundary condition $u(0) = 0$, we get $u_{outer} = 0$.

1.2 The case with $f = 0.5$ and $U = \pm 1$

First, consider first the case with $f = 0.5$ and $U = 1$. This is the same as the previous case, except for the fact that $f = 0.5$. Again, we can represent the solution as the sum of an inner solution and an outer solution. The inner solution is proportional to the solution given in (5). The outer solution is given by solving $\frac{d}{dx}u_{outer} = f/U = 0.5$ with $u_{outer}(0) = 0$, which has the solution $u_{outer} = 0.5\,x$. Combining the two solutions and applying the boundary condition at $x = 1$ gives

$$\begin{aligned} u(x) &= u_{inner} + u_{outer} && (8)\\ &= 0.5\,\frac{e^{x/\varepsilon} - 1}{e^{1/\varepsilon} - 1} + 0.5\,x\ . && (9) \end{aligned}$$

It is readily seen that this solution satisfies both the differential equation (1) and the boundary conditions (2) and (3).

Next, consider the case with $f = 0.5$ and $U = -1$, i.e., the "wind" is blowing from right to left. We thus expect the solution to exhibit a boundary layer of thickness ε near $x = 0$.

Following the same procedure as before, we express the total solution as

$$\begin{aligned} u(x) &= u_{inner} + u_{outer} && (10)\\ &= 1.5\,\frac{1 - e^{-x/\varepsilon}}{1 - e^{-1/\varepsilon}} - 0.5\,x\ . && (11) \end{aligned}$$

1.3 Weak formulation

Let us now give the weak formulation of the one-dimensional convection-diffusion problem (1)-(3). To this end, we first define the function spaces

$$\begin{aligned} X^D &= \{v \in H^1(\Omega) \mid v(0) = 0;\, v(1) = 1\}\ , && (12)\\ X &= \{v \in H^1(\Omega) \mid v(0) = 0;\, v(1) = 0\} \equiv H_0^1(\Omega). && (13) \end{aligned}$$

The weak form of (1)-(3) can then be expressed as: Find $u \in X^D$ such that

$$a(u, v) = l(v) \qquad \forall v \in X\ , \tag{14}$$

with

$$\begin{aligned} a(w, v) &= \int_0^1 (\kappa\, w_x v_x + U\, w_x v)\, dx && (15)\\ l(v) &= \int_0^1 f\, v\, dx\ . && (16) \end{aligned}$$

When $U = 0$, we recover the Poisson problem. Note that the bilinear form $a(\cdot, \cdot)$ is nonsymmetric when $U \neq 0$.

1.4 Discrete formulation

Our discrete formulation is based upon the weak formulation. In particular, we assume that we use K finite elements, T_h^k, $k = 1, ..., K$, and that the numerical solution is approximated as a first-order polynomial over each element (i.e., we use linear elements).

Mathematically, we define our finite-dimensional subspaces as

$$X_h^D = \{v \in X^D \mid v_{|_{T_h^k}} \in I\!P_1(T_h^k),\ k = 1, ..., K\} \ , \tag{17}$$

$$X_h = \{v \in X \mid v_{|_{T_h^k}} \in I\!P_1(T_h^k),\ k = 1, ..., K\} \ . \tag{18}$$

The discrete problem can now be stated as: Find $u_h \in X_h^D$ such that

$$a(u_h, v) = l(v) \qquad \forall v \in X_h \ . \tag{19}$$

Hence, our numerical solution is piecewise linear, it is continuous across the elements, and it satisfies the prescribed Dirichlet boundary conditions.

1.5 Algebraic formulation

As usual, we choose nodal bases for X_h^D and X_h:

$$\forall v \in X_h^D \,, \qquad v(x) = \sum_{i=1}^{N} v_i \, \phi_i(x) + \phi_{N+1} \ , \tag{20}$$

$$\forall v \in X_h \,, \qquad v(x) = \sum_{i=1}^{N} v_i \, \phi_i(x) \ . \tag{21}$$

$$\tag{22}$$

A few remarks: First, note that $K = N + 1$. Second, note that we add the (hat) basis function ϕ_{N+1} associated with the right end point because of the inhomogenous Dirichlet boundary condition $u(x = 1) = 1$. Third, note that, $\forall v \in X_h$, $v(x_0) = v(x_{N+1}) = 0$.

Inserting these bases into the discrete formulation, we arrive at a set of algebraic equations

$$\underline{A}_h \, \underline{u}_h = \underline{F}_h \ , \tag{23}$$

where

$$u_h(x) = \sum_{i=1}^{N} u_{hi} \, \phi_i(x) + \phi_{N+1} \tag{24}$$

and

$$\underline{u}_h = [u_{h1}, u_{h2}, ..., u_{hN}]^T \ . \tag{25}$$

Because we are using a nodal basis, the unknowns represent the numerical solution at the *internal* global points x_i, $i = 1, ..., N$.

We assemble the global matrix $\underline{A}_h$ by adding up all the elemental contributions. The element matrix $\underline{A}_h^k$ associated with the bilinear form (15) can be expressed as

$$\underline{A}_h^k = \frac{\kappa}{h^k} \begin{pmatrix} 1 & -1 \\ -1 & 1 \end{pmatrix} + \frac{U}{2} \begin{pmatrix} -1 & 1 \\ -1 & 1 \end{pmatrix} . \tag{26}$$

Here, h^k is the length of element T_h^k, $k = 1, ..., K$.

The (local) grid Peclet number is defined as

$$P_g = Pe_g^k = \frac{U\, h^k}{\kappa} . \tag{27}$$

Note that the grid Peclet must be thought of as a *locally* defined quantity for a nonuniform grid. We know that, on a uniform grid, the numerical solution can exhibit oscillations when the grid Peclet number is greater than 2. In order to avoid having to resolve a thin boundary layer, but still being able to resolve the outer solution, it is common to use upwinding. In the finite element context, this is achieved by adding a controlled amount of diffusion in the streamwise direction. In particular, in $I\!R^1$, instead of using the physical thermal conductivity κ, we use the modified conductivity

$$\tilde{\kappa} = \kappa + U\, \frac{h^k}{2} \tag{28}$$

on each element. This corresponds to a modified diffusivity

$$\tilde{\varepsilon} = \varepsilon + \frac{h^k}{2} . \tag{29}$$

The boundary layer thickness will thus be $\tilde{\varepsilon}$ instead of ε. For a fixed discretization, the numerical solution will have a boundary layer of no less than $\frac{h^k}{2}$ even if $\varepsilon \to 0$. In this case, the numerical error will be $\mathcal{O}(1)$ in the vicinity of the boundary layer. On the other hand, we obtain a stable solution. If f varies slowly, the outer solution will typically be well resolved.

1.6 Extension to two and three dimensions

The finite element procedure just described can be extended to two and three space dimensions. The key ingredients are:

- Use the weak form as a point of departure for the discretization.
- Decompose the domain into elements (triangles, squares, etc.).
- Construct all the elemental matrices $\underline{A}_h^k$, $k = 1, ..., K$. For each element, modify the diffusivity in the *streamwise* direction only, and similar to the one-dimensional procedure described above. In order to achieve this, we need to introduce a tensor-diffusivity, i.e., a diffusivity which depends on the spatial direction.
- Assemble the global matrix $\underline{A}_h$ and the global right hand side $\underline{F}_h$ from the elemental contributions, and by using a local-to-global numbering scheme.
- Solve the system of algebraic equations, $\underline{A}_h \, \underline{u}_h = \underline{F}_h$, for the nodal values $\underline{u}_h$.

1.7 Solution method

We now comment on solving the system of algebraic equations

$$\underline{A}_h \, \underline{u}_h = \underline{F}_h \tag{30}$$

for the nodal values $\underline{u}_h$, where $\underline{A}_h$ is the discrete convection-diffusion operator (non-symmetric), and $\underline{F}_h$ is a known right hand side.

If we use a *direct solver*, we can use a banded solver or a sparse solver for non-symmetric matrices. Note that pivoting may be necessary.

If we use an *iterative solver*, we cannot use the conjugate gradient method because $\underline{A}_h$ is not symmetric. However, we can use a solver like the GMRES (General Minimum RESidual) method. Irrespective of which type of iterative solver we use, we will typically need a good preconditioner in order to limit the number of iterations, or in order to obtain convergence at all. Note that, if the Peclet number is high (i.e., convection-dominated problems), the need for having a good preconditioner increases.

1.8 Numerical results

We now discuss a series of numerical results obtained for the one-dimensional convection-diffusion problem (1)-(3). We note that almost all the numerical solutions are obtained using $K = 20$ linear finite elements, i.e., $N = 19$.

We start with the case $f = 0$ and $U = 1$. In Figure 1 and Figure 2, the Peclet number $P = 4$, while the grid Peclet number $P_g = 0.2$ (uniform grid). Since $P_g \ll 2$, upwinding is not really necessary for stability. Figure 1 shows that the numerical solution is very close to the analytical solution, while upwinding thickens the boundary layer with $h^k/2 = 0.025$; see Figure 2.

In Figure 3 and Figure 4, we show similar results for $P = 20$ and $P_g = 1$. Again, no upwinding is needed for stability. In this case, the boundary layer thickness is $\varepsilon = 0.05$. Adding upwinding increases the boundary layer thickness to $\tilde{\varepsilon} = \varepsilon + h^k/2 = 0.05 + 0.025 = 0.75$, i.e., a 50% relative increase.

In Figure 5 and Figure 6, the Peclet number is increased to $P = 100$, while using the same grid as before; hence, the grid Peclet number is now $P_g = 5$. As expected, we now get oscillations in the numerical solution without upwinding. Adding upwinding will fatten the boundary layer, while giving an accurate outer solution $u_{outer} = 0$.

A more extreme situation is shown in Figure 7 and Figure 8 where $P = 500$ and $P_g = 25 \gg 1$. We now get oscillations over the entire computational domain. Adding upwinding gives a stable solution with no oscillations. In this case, the error near $x = 1$ is large, while the outer solution $u_{outer} = 0$ is well represented.

From the previous results, it appears natural to consider the use of a nonuniform grid. In particular, let the global nodes be be distributed as follows

$$x_i = \frac{1}{2}\,(1 - cos(\frac{\pi\, i}{N+1}))\;\; i = 0, 1, ..., N+1. \tag{31}$$

This compares with a uniform grid where the global nodes are given as

$$x_i = i\frac{1}{N+1}\;\; i = 0, 1, ..., N+1. \tag{32}$$

The length (or diameter) of each element T_h^k is given by

$$h^k = x_k - x_{k-1}\;\; . \tag{33}$$

For the nonuniform distribution (31), the element size is smallest near the boundaries $x = 0$ and $x = 1$, while the element size is biggest in the middle of the domain. For the uniform distribution (32), all the elements have the same length $h = 1/(N+1)$.

We reconsider the case $P = 100$, but now using a nonuniform grid. The number of grid points is the same as before. If we compare the numerical solution in Figure 9 with the earlier solution in Figure 5, we notice a great

improvement. This can partly be understood by noticing that the local grid Peclet number is now less than 2 near the boundaries; see Figure 10.

We now discuss some numerical results for the case $f = 0.5$. In order to limit the discussion, we consider the case $P = 100$. First, let $U = 1$. Figure 11 shows the numerical solution in the case of using a uniform grid. As expected, we get oscillations near the right boundary. Adding upwinding removes the oscillations, see Figure 12, but fattens the boundary layer; however, the outer solution is well resolved.

Next, we consider the case $P = 100$ and $U = -1$. We arrive at the same conclusion as in the previous case; see Figure 13 and Figure 14.

Again, we consider the cases $P = 100$ and $U = \pm 1$, but now using a nonuniform grid given by (31). For the same number of elements as before, we see a significant improvement; see Figure 15 and Figure 16.

For a *fixed* number of elements, we see that that we can improve the numerical results by considering a nonuniform grid which takes into account the particular solution structure. In addition, we can also apply upwinding. We remark that we can, of course, also improve all the previous results by increasing the number of elements (with an associated increase in the computational cost). As an example, we show in Figure 17 the numerical solution for the case $P = 100$ and when using a uniform grid with $K = 100$ elements (i.e., 5 times as many elements as in Figure 5 and Figure 9). As expected, the numerical solution is now resolved over the entire domain.

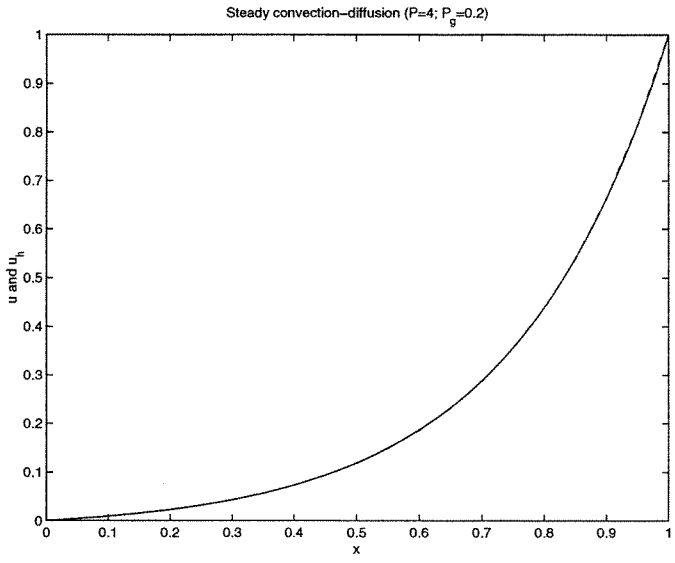

Figure 1: A comparison between the exact solution (solid line) and the finite element solution (dashed line) in the case of using a uniform grid with $K = 20$ elements, $\kappa = 0.25$, $U = 1$ and $f = 0$. The Peclet number is $P = 4$, while the grid Peclet number is $P_g = 0.2$. No upwinding is applied.

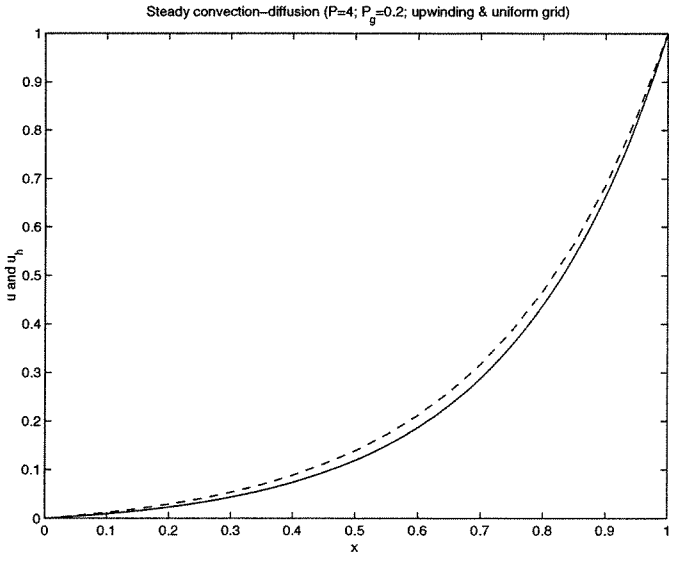

Figure 2: Same case as described above, but now using upwinding.

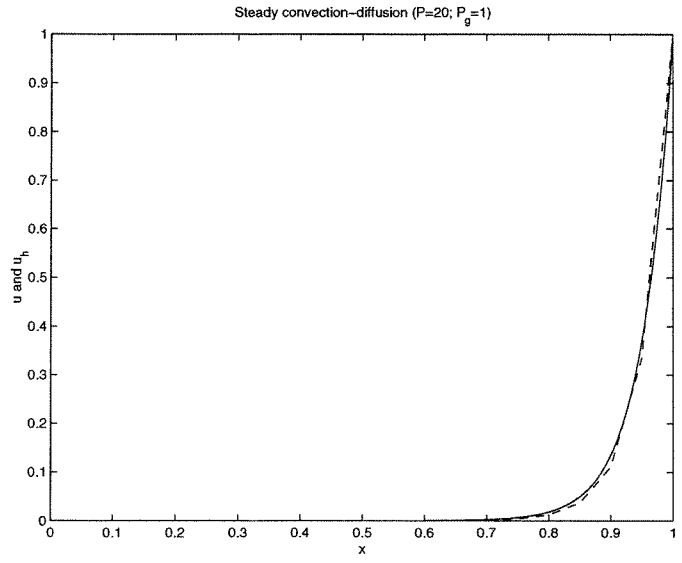

Figure 3: A comparison between the exact solution (solid line) and the finite element solution (dashed line) in the case of using a uniform grid with $K = 20$ elements, $\kappa = 0.05$, $U = 1$ and $f = 0$. The Peclet number is $P = 20$, while the grid Peclet number is $P_g = 1$. No upwinding is applied.

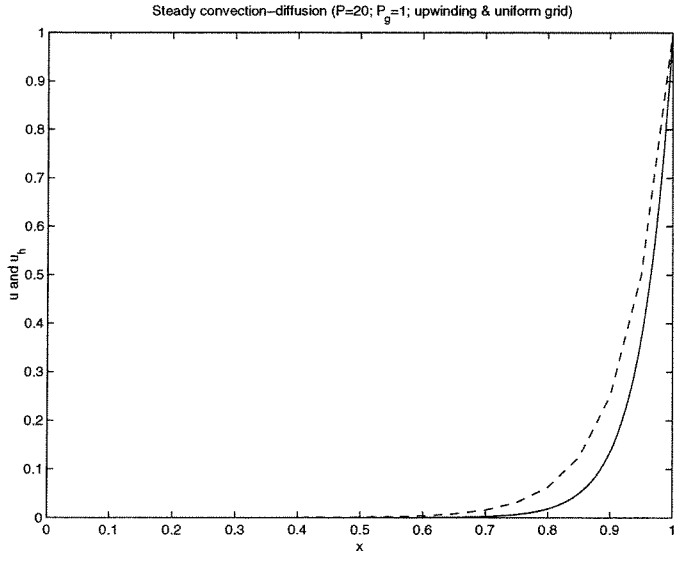

Figure 4: Same case as described above, but now using upwinding.

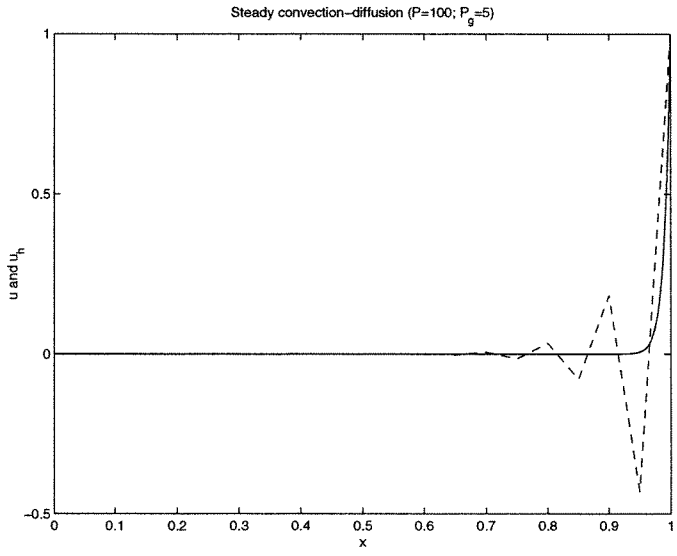

Figure 5: A comparison between the exact solution (solid line) and the finite element solution (dashed line) in the case of using a uniform grid with $K = 20$ elements, $\kappa = 0.01$, $U = 1$ and $f = 0$. The Peclet number is $P = 100$, while the grid Peclet number is $P_g = 5$. No upwinding is applied.

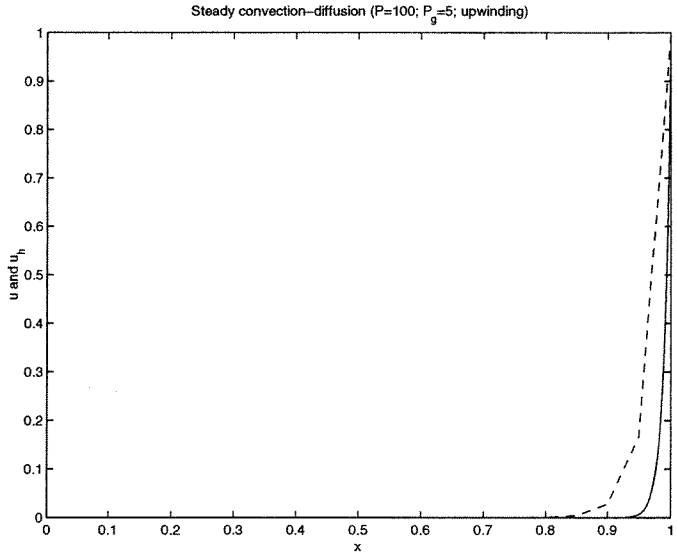

Figure 6: Same case as described above, but now using upwinding.

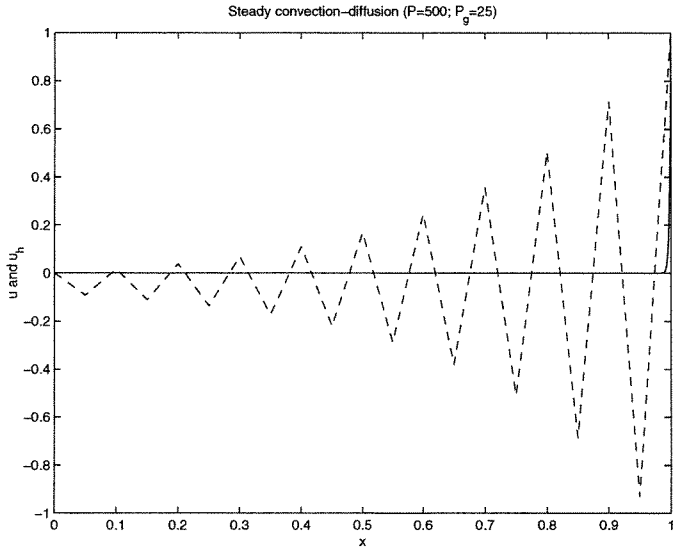

Figure 7: A comparison between the exact solution (solid line) and the finite element solution (dashed line) in the case of using a uniform grid with $K = 20$ elements, $\kappa = 0.002$, $U = 1$ and $f = 0$. The Peclet number is $P = 500$, while the grid Peclet number is $P_g = 25$. No upwinding is applied.

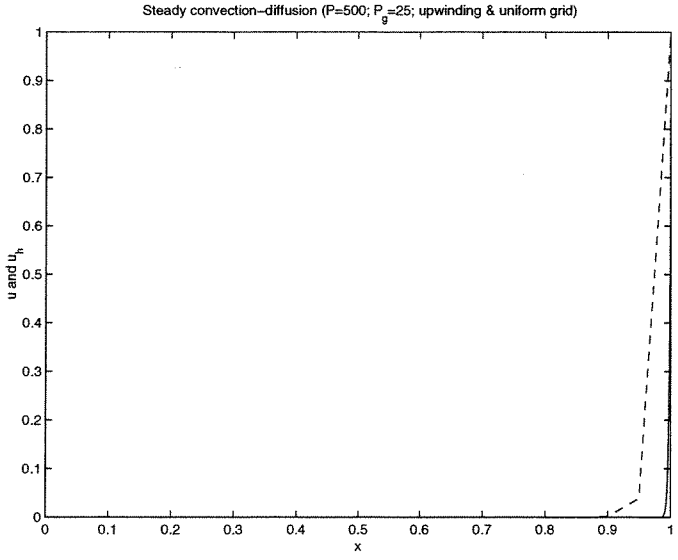

Figure 8: Same case as described above, but now using upwinding.

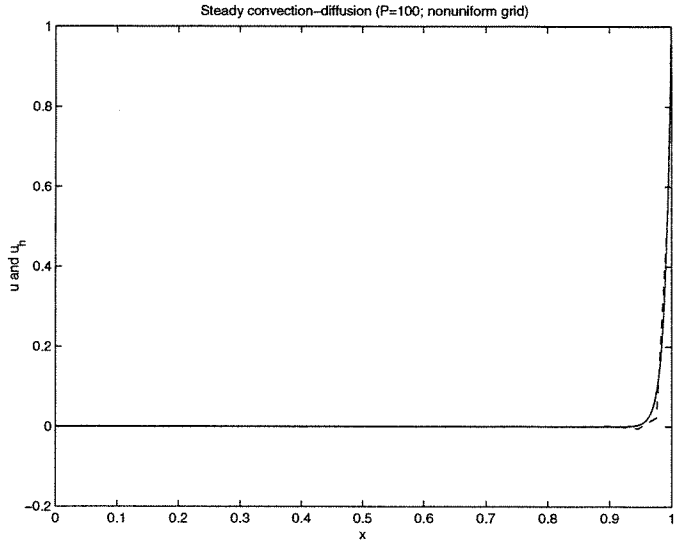

Figure 9: A comparison between the exact solution (solid line) and the finite element solution (dashed line) in the case of using a nonuniform grid with $K = 20$ elements, $\kappa = 0.01$, $U = 1$ and $f = 0$. The Peclet number is $P = 100$, while the grid Peclet number is variable (see below). No upwinding is applied.

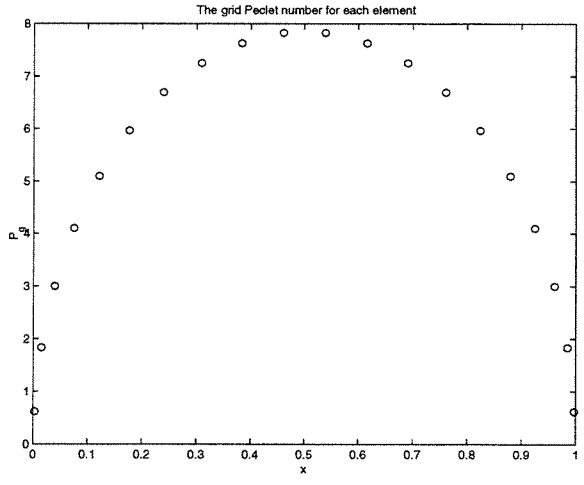

Figure 10: A plot of the grid Peclet number in the case of using a nonuniform grid. The grid Peclet number is marked as a circle located at the center of each element. The grid Peclet number varies between approximately 8 in the center of the domain to less than 2 near the boundaries.

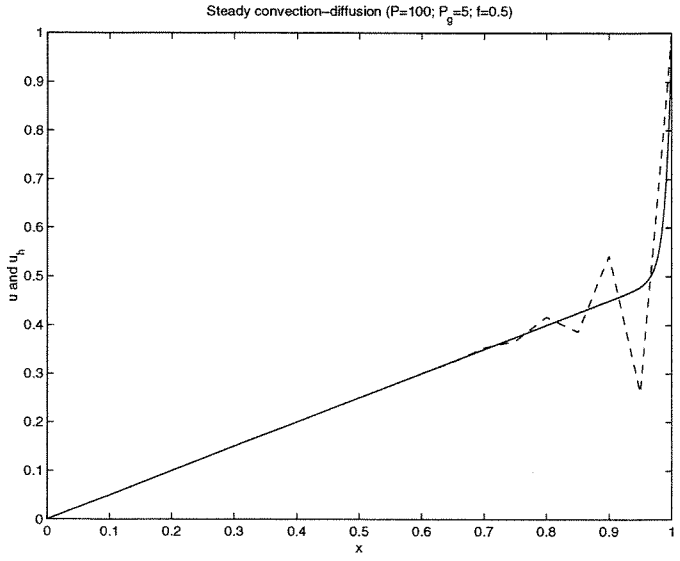

Figure 11: A comparison between the exact solution (solid line) and the finite element solution (dashed line) in the case of using a uniform grid with $K = 20$ elements, $\kappa = 0.01$, $U = 1$ and $f = 0.5$. The Peclet number is $P = 100$, while the grid Peclet number is $P_g = 5$. No upwinding is applied.

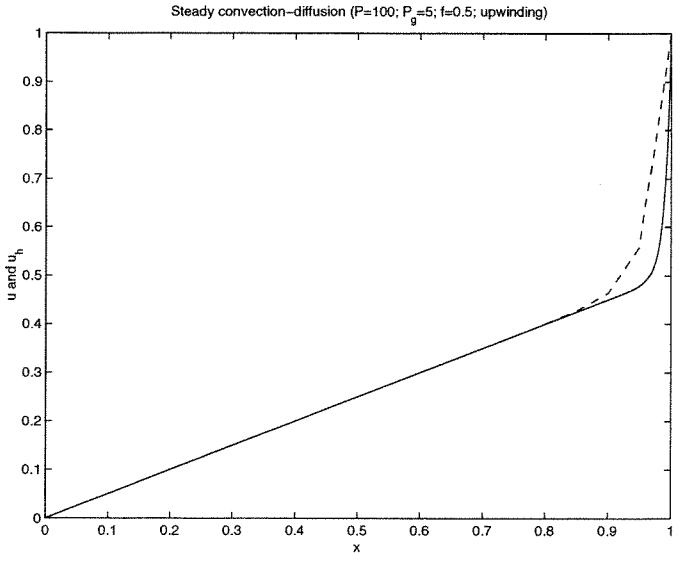

Figure 12: Same case as described above, but now using upwinding.

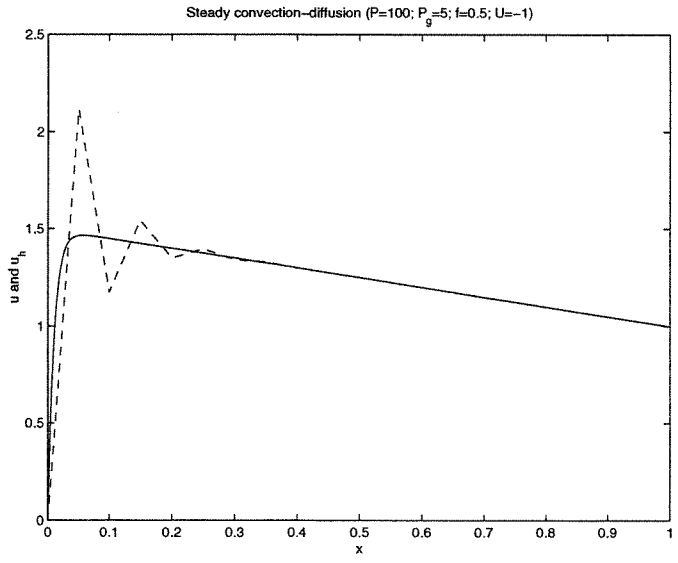

Figure 13: A comparison between the exact solution (solid line) and the finite element solution (dashed line) in the case of using a uniform grid with $K = 20$ elements, $\kappa = 0.01$, $U = -1$ and $f = 0.5$. The Peclet number is $P = 100$, while the grid Peclet number is $P_g = 5$. No upwinding is applied.

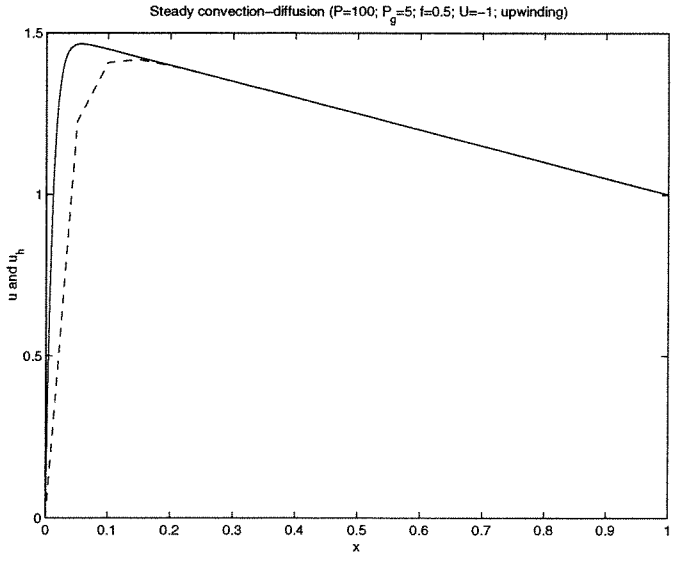

Figure 14: Same case as described above, but now using upwinding.

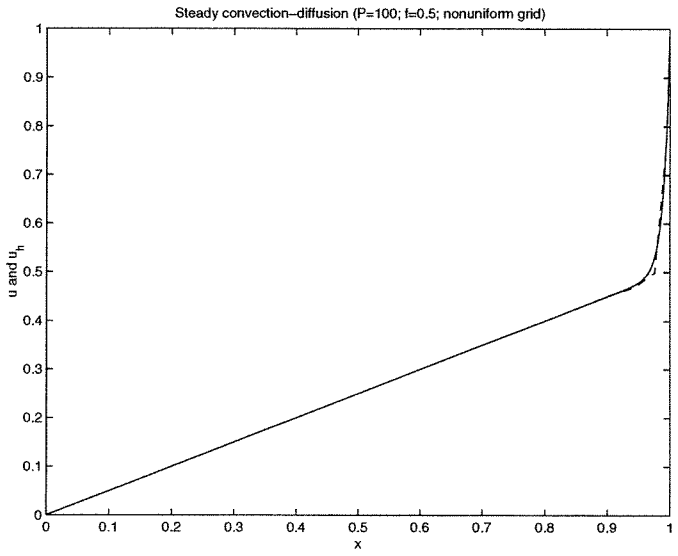

Figure 15: A comparison between the exact solution (solid line) and the finite element solution (dashed line) in the case of using a nonuniform grid with $K = 20$ elements, $\kappa = 0.01$, $U = 1$ and $f = 0.5$. The Peclet number is $P = 100$, while the grid Peclet number is variable; see Figure 10. No upwinding is applied.

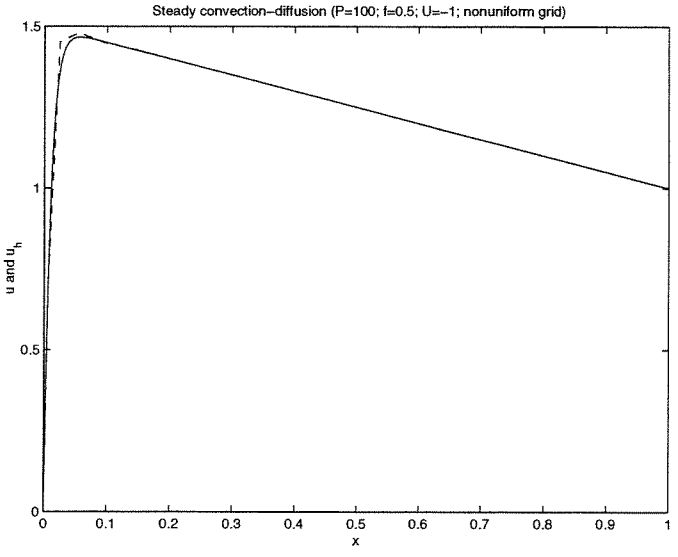

Figure 16: Same case as described above, but with $U = -1$.

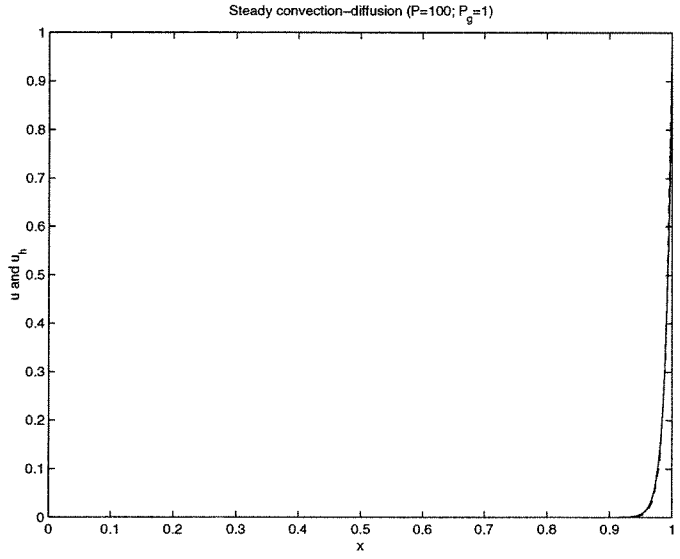

Figure 17: A comparison between the exact solution (solid line) and the finite element solution (dashed line) in the case of using a uniform grid with $K = 100$ elements, $\kappa = 0.01$, $U = 1$ and $f = 0$. The Peclet number is $P = 100$, while the grid Peclet number is $P_g = 1$. No upwinding is applied.